Determining radius of influence of the face in EPB shield tunneling by finite difference method.

S. Gharehdash, M. Barzegar
Department of Mining and Metallurgical Engineering, Amirkabir University of Technology, Tehran, Iran.
M. Sharifzadeh
Department of Mining Engineering, Curtin University, Perth, Western Australia.

ABSTRACT: For the purpose of understanding the three-dimensional behavior of face tunnel, a three-dimensional finite difference simulation model, which includes all relevant shield tunneling components and allows for the modeling of the step-by-step construction process of the tunnel advance. The soil-structure interaction in shield tunneling is investigated by numerical solution. The results of three-dimensional ground displacements and stress pattern around a tunnel face and at the ground surface are examined. Results obtained from these analyses indicate that the general three-dimensional stress and displacement patterns around a tunnel heading are very different from that at the plane strain transverse section. The distance required for the ground displacement to reach the plane strain condition will depend on the amount of plasticity developed around the tunnel opening. Consequently, face is the most important zone for the design engineer in EPB tunneling.

1 INTRODUCTION

A variety of theoretical and numerical models for estimation of the minimum required support pressure have been proposed. Most analytical results are based on the limit equilibrium method and the limit analysis method. In addition, numerical and experimental methods are also adopted to study the failure mechanism of a tunnel face and surface settlement due to tunnelling [Li, et al., Guglielme, et al., Subrin, et al., Renpeng, et al].

These movements are the result of complex actions between the ground and the tunneling process. The performance of a tunnel is greatly influenced by the excavation and support procedure, as well as by the initial and long term ground behavior. A better understanding of these influences and proper consideration of their effects on support design and installation will lead to more efficient and economic tunnel construction [Jiang, et al., Kirsch, et al].

The goal of this study is to analyse the different stages of the excavation works and of the interaction between the ground and the tunnel face, in order to propose a correct numerical modeling of all these physical phenomena. Particular attention will be focused on the influence of the varying face support pressure on the general three-dimensional non-linear soil movements and ground reactions both around the tunnel face and at the ground surface.

Earth pressure balance shields provide continuous support of the tunnel face using freshly excavated soil, which completely fills up the work chamber under pressure. The supporting pressure is achieved through control of the incoming and outgoing materials in the chamber, i.e., through regulation of the screw conveyor rotation and the excavation advance rate. The earth pressure of working face is classified into two kinds of types. The first class is active earth pressure, which is from the active action of earth pressure to the shield structure if the thrust force of shield is less than composite force of active earth pressure. The second class is passive earth pressure, which is from the active action of shield structure to the earth mass in front of working face if the thrust force of shield is greater than composite force of active earth pressure. To investigate the behavior of the Mashhad metro tunnel face

subjected to support pressures (ranging from 10% to 200% of lateral earth pressure,σ_T/σ_y) a numerical study was carried out to examine the effect of face support pressure on the size of the disturbed zone in proximity to the face.

1.1 *Numerical modelling of face stability*

It is generally recognized that numerical modeling of the construction sequence of a soft ground shield tunnel is a complex task since the actual field situation is truly three-dimensional, involves non-linear soil behavior and is, to a large extent, highly indeterminate since it depends on the construction procedure and the experience of the workmen controlling the tunneling machine. In particular, the size of the disturbed zone around the tunnel and the extent of overcutting which results from the use of a closed face tunneling machine are primarily related to workmanship and cannot be precisely determined prior to construction. Thus, any analysis no matter how simple or sophisticated, must involve some empirically determined factors to account for workmanship issues. In view of this, the aim of this study is not to perform an analysis which involves full simulation of shallow tunnel construction process. Rather, a number of approaches were adopted which attempt to investigated the general three-dimensional non-linear soil movements and ground reactions both around the tunnel face and at the ground surface. In order to demonstrate the fundamental three-dimensional aspect of the problem a comprehensive numerical study was conducted employing the FLAC3D code (Itasca Consulting Group, 2006). The model dimensions were selected large enough to avoid boundary effects. The soil layers are assumed to be an elasto-plastic material conforming to the Mohr-Coulomb failure criteria. The tunnel has a diameter of D= 9.5 m and a cover depth of 1.17m. It is assumed the tunnel is driven by means of an earth pressure balance TBM in soft soil. Figure 1 shows the different components of the constructed numerical model. Neglecting the deformations of the shield skin, the TBM was modeled as a rigid contact body. The length of the shield was assumed to be 10 m with regard to the TBM specifications. The step-by-step excavation process was modeled by repeated rezoning of the element mesh at the cutting face and repeated insertion of elements representing the tunnel lining and the tail void grout, respectively.

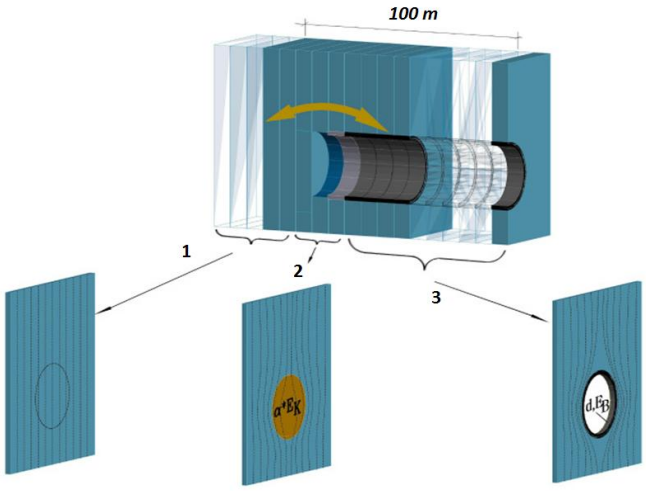

Figure 1. 3-D finite difference mesh, Representation of the different shield tunneling components in the model.

Furthermore, the boundary conditions for the face support and the grouting pressure were adjusted according to the progress of the simulated tunnel advance. The elements of the grout are directly connected to the elements of the tunnel lining on the inner side and the soil on the outer side. The concrete lining was, therefore, modeled in a simplified way as a continuous, isotropic, elastic tube. The conditioned muck pressure in the excavation chamber is assumed to vary linearly in the vertical direction according to the assumed bulk density of 13 KN/m3 for the muck in the excavation chamber. According to the site investigation results, soils can be differentiated into a number of well-defined strata based on physical properties and soil types, as illustrated in Table 1. Grouting pressure distribution is complicated. Uneven grouting pressure would cause segment dislocation and even crack. The grouting pressure was modeled by pore pressure boundary conditions on the grout element nodes at the shield tail according to the assumed grouting pressure with a variation of 15 KN/m2/m over the height. In table 2 the vertical soil pressures at the largest and shallowest depths are presented. This in order to get an idea of the pressures needed to inject the annular void during excavation. The tunnel is mainly hosted by highly compressible and silty clay and sandy deposits. The minimal grout pressure should at least be 2 bar more than the prevailing soil pressures. In this paper, P_{in} denotes

grouting pressure. In order to reflect general situation, P_{in1} was assumed to be ±3.5 bar, and P_{in2} to be ±5.2 bar. Table 3 shows the mechanical properties of encountered materials used in the model.

Table 1. Physical and mechanical properties various soil layers along the tunnel

Layer	Soil type	Water content w	Plasticity index I_p	Earth pressure coefficient at rest K_o	Undrained shear strength C_u	Young's Modulus E	Poisson's ratio ν	Friction angle φ_{cu}	Cohesion C_{cu}	Unit weight γ_{bulk}
		(%)	-	-	kPa	MPa	-	degree	kPa	kN/m^2
I	SC-SM	44	17	0.43	21	80	0.3	35	0	19
II	GC-GM	30	15	0.36	-z	100	0.2	40	11	19
III	CL-ML	35	21	0.61	-z	30	0.3	20	25	18

Table 2. Boundary pressures for grout injection

Tunnel	*Top* *Bottom*
Depth (m)	10.67 19.795
σ_v (kN/m2)	149 318
Grout pressure (bar)	3.5 5.2

Table 3. Material models and parameters used.

Material Type	Constitutive model	Thickness	E (Bulk Modulus)	ν (Poisson's ratio)	φ (Friction angle)	C (Cohesion)
		Cm	MPa	-	Degree	kPa
Shield	elastic	10	210000	0.17	-	-
Grout	Mohr-coulomb	12	40	0.25	35	600
Lining	elastic	35	30000	0.2	-	-

1.2 *Simulation result*

It is assumed that a normal pressure with intensity 1000 kPa is instantaneously applied to the face, which generate not only a quasi-longitudinal, as in isotropic media, but also quasi-shear stress with axially symmetrical face surfaces. After interaction with the face tunnel, also only two types of each of axisymmetric normal and shear stress in the plane of axial cross-section are initiated. In Figure 2 the lines of fronts of the face are shown for the selected face support pressure. It can be seen, that the intensity of the normal stress exceeds the intensities of the shear stress. In this Figures, (1) is an undisturbed zone, where the ground is not yet affected by the passage of the face. (2) is a tunnel face or transition zone, corresponding to the radius of influence of the face, in which its presence has a considerable effect. (3) is a stabilization zone, where the face no longer has any influence and the situation tends to stabilize (if possible), (x in horizontal axis is distance from the tunnel face).

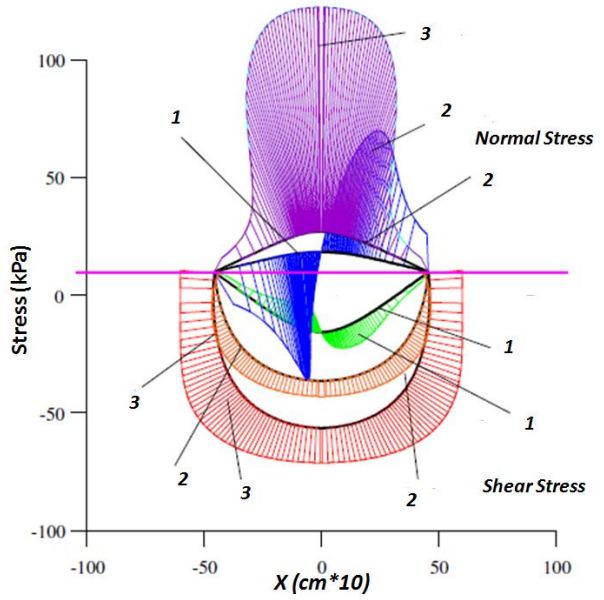

Figure 2. Stress patterns in different zones in tunneling process.

In Figure 3, the results of the construction of a tunneling process are demonstrated. In consequence of this, the intensity of stress deflect their directions and the face support pressure becomes curvilinear. Thereupon after interaction of the transformed tunneling process, the phenomenon of the face influence is completed.

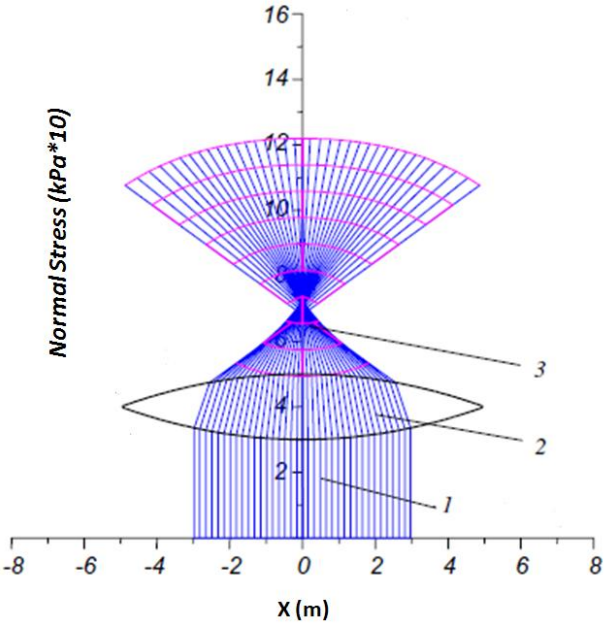

Figure 3.Normal stress patterns in different zones in tunneling process.

Besides, it is impossible to calculate the stress intensity at the excavation process, because the stress divergence tends to zero at them (see Figure 4). For this reason the stress increases endlessly and the stress intensity acquires infinite value.

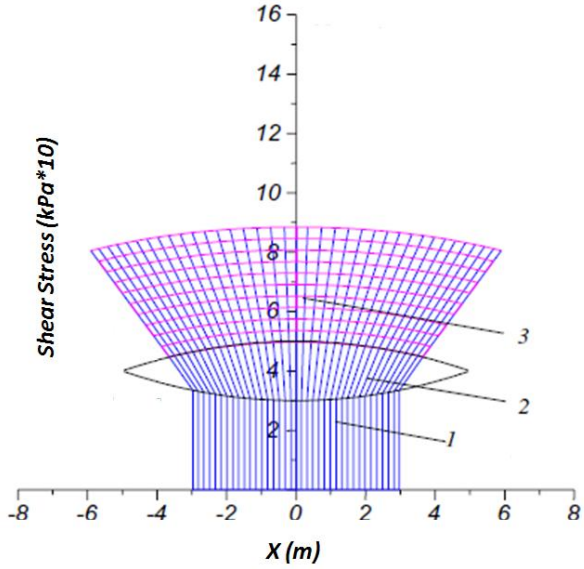

Figure 4. Normal stress patterns in different zones in tunneling process.

Stress paths along the tunnel boundaries and at the tunnel face were analysed along the tunnel boundary ahead of the face for several lines running parallel to the tunnel axis. The three-dimensional mesh was assembled so that these lines would coincide with the tunnel roof and walls, both on the tunnel boundary and along a parallel line 1m into the soil, and along the centerline of the tunnel axis ahead of the working face. Based on this analysis methodology, several series of model runs were performed focusing on the influence of face influence with respect to the face support pressure. For each model run in this series, results are presented. Figure 5, provides plots of the deviatoric stress contours along the longitudinal tunnel profile. Three characteristic zones can be identified during tunnel advance in an lined tunnel. An undisturbed zone, a tunnel face or transition zone and a stabilization zone.

It is important to observe that in passing from the undisturbed zone to the stabilization zone, the medium passes from a triaxial to a plane stress state and that the face zone is where this transition takes place. Consequently, this is the

most important zone for the design engineer. It is here that the action of excavation disturbs the medium and it is on this zone that all the attention of the design engineer must be focused for proper study of a tunnel. It is not possible to achieve this without employing three dimensional analysis approaches (see, Figure 5).

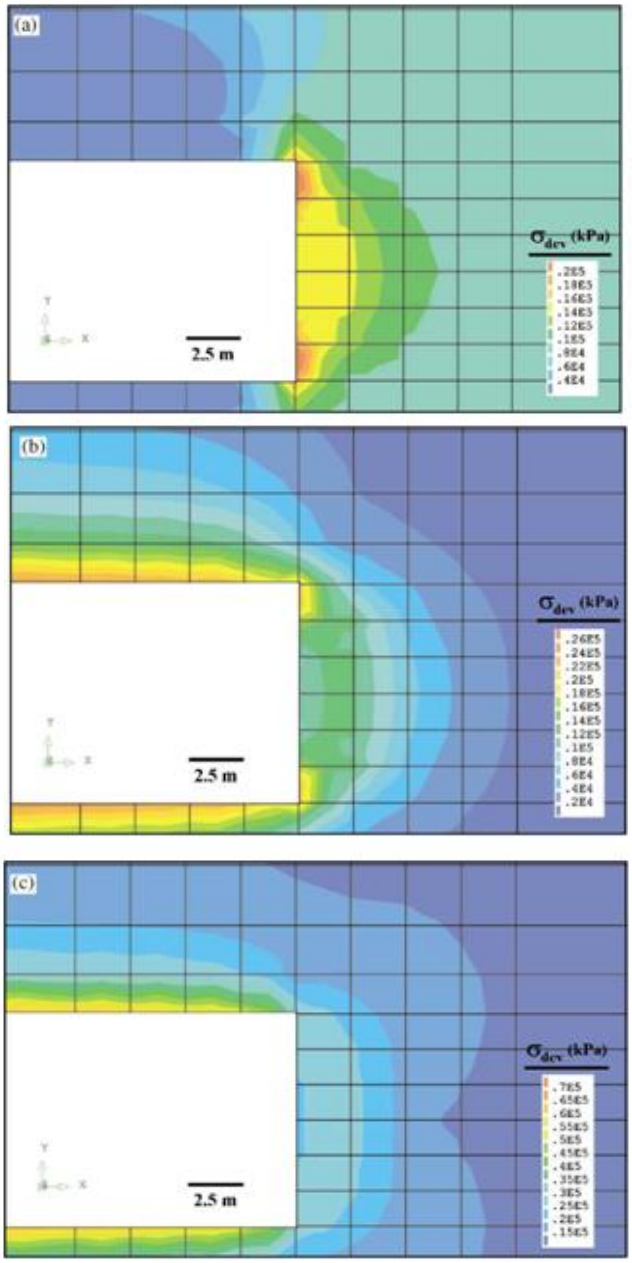

Figure 5. Plots of the deviatoric stress contours, along the longitudinal tunnel profile (i.e. parallel to the tunnel axis) (a) zone 2; (b) zone 3; (c) zone 1.

A comparison between deviatoric stresses at the tunnel face calculated assuming plastic yielding are shown in Figure 6, for the different face support pressure. These results show that the stresses in the face zone are significantly lower along the tunnel roof, where the zone of yield extends approximately 2 m, or 0.2 tunnel diameters, from the tunnel boundary. Moving outwards from the yielded zone, i.e. between 2 to 5 m from the tunnel boundary, stresses are higher than in the face zone due to the shedding of stresses outwards from the inner yielded elements (see Figure 6). Numerical analysis in Figures 5 and 6 indicates that no less than 30% of the total convergence deformation produced in a given section of tunnel develops before the face arrives. It follows that the ground ahead of the face is the first to deform and that it is only after it has deformed that convergence of the cavity is produced (see Figure 5). It also follows that the convergence changes taken inside the tunnel only represent a part of the total deformation phenomenon that affects the medium (see Figure 6). The design engineer must focus his attention and within which the passage from a triaxial to a plane stress state occurs (the face or transition zone); proper study of a tunnel therefore requires three dimensional methods of calculation and not just plane methods.

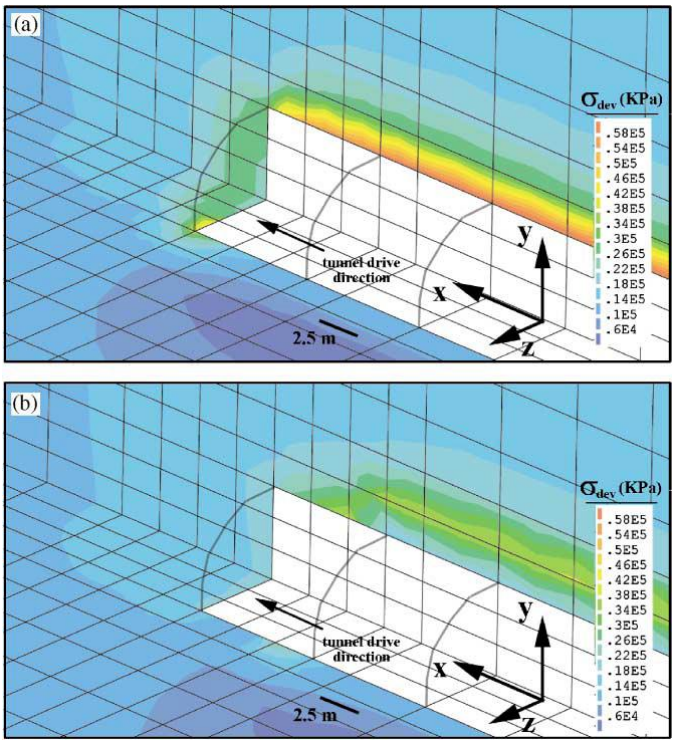

Figure 6. Plots of the deviatoric stress contours, along the longitudinal tunnel profile assuming different face support pressure.

.

Figure 7. demonstrates the accumulation of plastic strain in the soil at the tunnel face advances towards two fixed monitoring planes for the modeling. However, this analysis only considers temporal changes to the soil resulting from increased stress magnitudes. Conceptually, and of equal interest, is how the directional propagation of the stress-induced in the damage zone contribute to soil strength degradation and resulting failure mechanism.

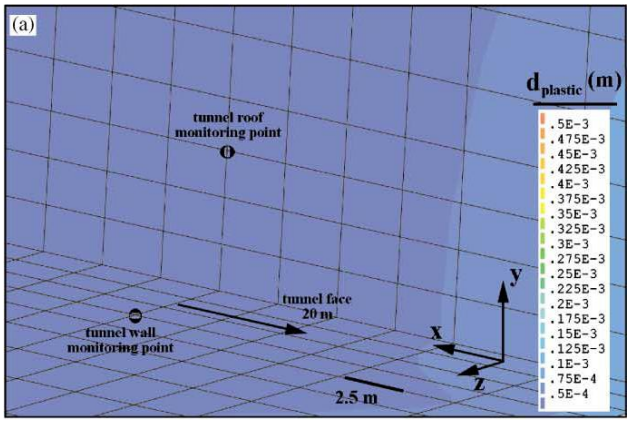

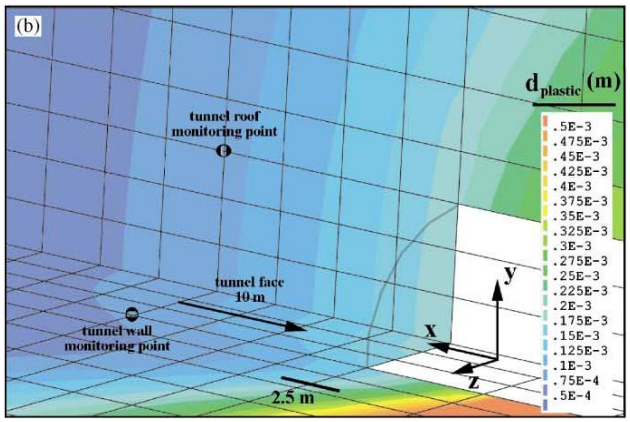

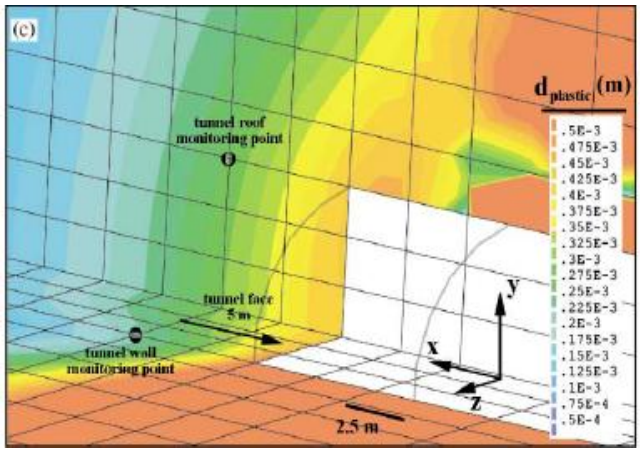

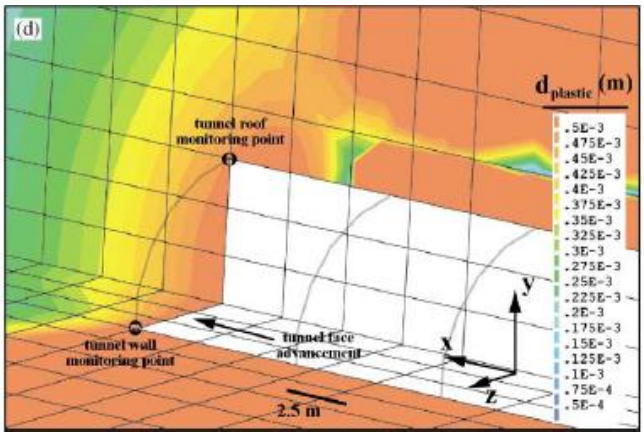

Figure 7. Contours of cumulative plastic displacements during advancement of the tunnel face relative to the position of fixed monitoring zones at: (a) 20m away; (b) 10m away; (c) 5m away; and (d) 0m away.

Figure 8, present the distribution of tensile yield elements in different zones of tunnel. It is seen that when the soil tensile strength is low, the difference of the yielding zone distribution is larger in zone 3. As the tensile strength increases, the yield zone patterns in the three zones gradually converge.

When advancing through ground in elasto-plastic conditions it is very important to keep excavations rates high and constant in order to avoid giving the tunnel time to deform. This prevents extrusion and preconvergence, which constitute the starting point of subsequent convergence of the cavity, from being triggered. What also emerged from the other experiences cited and similar cases was that: the failure of the tunnel is generally followed by the collapse of the cavity and it is very rare for the latter to be preceded by the former.

The results of the numerical analysis conducted during the construction of these tunnels demonstrated that deformation of the cavity can be controlled and substantially reduced by artificially regulating the rigidity of the tunnel face system with adequate face pressure properly designed and distributed between the ahead of the face and the cavity.

So the ground ahead of the face of a tunnel under construction can really be used as an effective instrument for stabilising a cavity in the short and long term (see Figures 8,9 and 10).

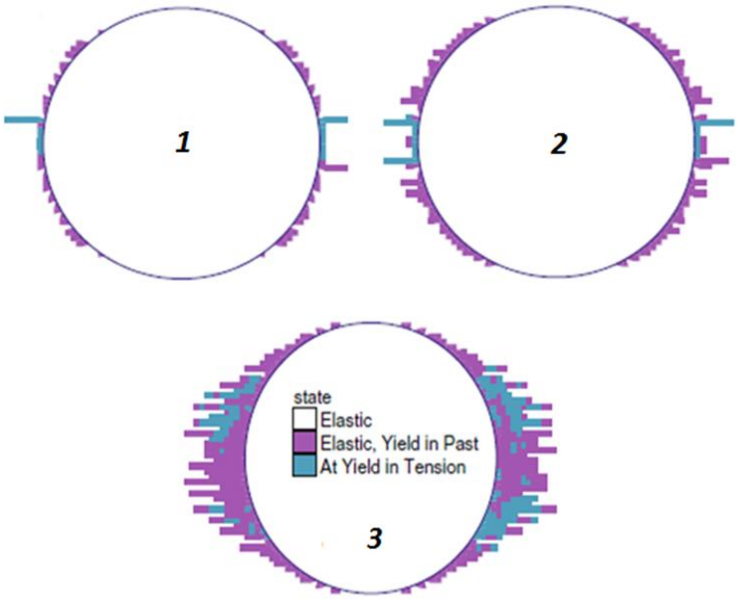

Figure 8. Comparison of tensile yielding zone distribution in different zones.

Figure 9, presents the simulation results, showing the shear yielding distribution around the tunnel.

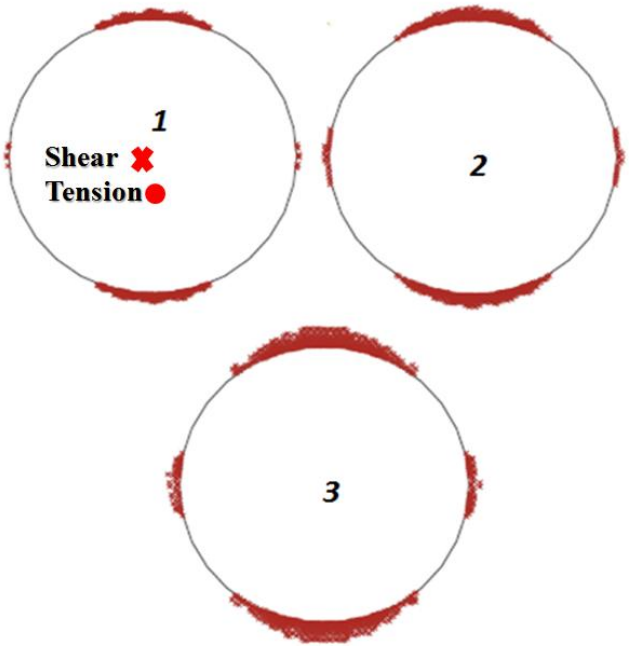

Figure 9. Comparison of shear yielding zone distribution in different zones.

Figure 10, presents the tensile and shear yielding zone distribution in passive and active pressure in tunnel face. Again, the tensile yielding zone is concentrated on the sidewalls and shear yielding zone on the roof and floor.

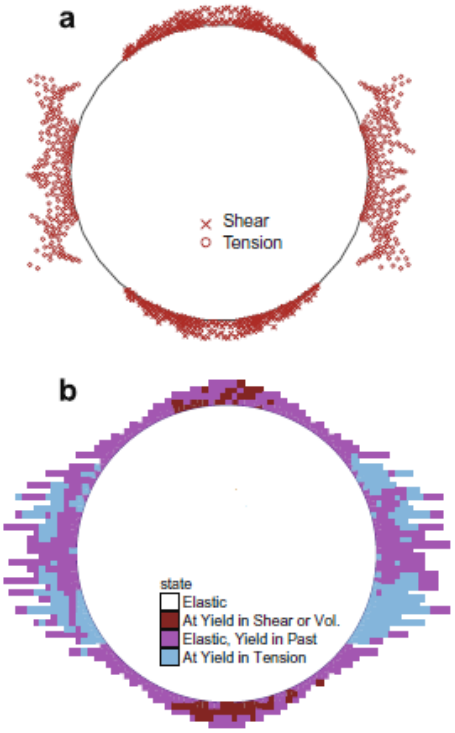

Figure 10. Comparison of tensile and shear yielding zone distribution in different zones.

The constructed model was sufficiently large to allow for any possible failure mechanism and to avoid any influence from the model boundaries. The focus of the analysis was on the radius of influence of the face around of the TBM. We therefore worked on the possibility of controlling the rigidity of the advance face tunnel in order to ascertain to what extent this would make it possible to control the deformation response of the tunnel.

The different soil layers are assumed to be elastic-perfectly plastic materials conforming to the Mohr-Coulomb criterion. The freshly excavated soil pressure acting on the tunnel face was considered as a linearly distributed pressure, which increases with depth according to the density of the conditioned muck in the excavation chamber. The initial conditioned muck pressure at the level of the center of the tunnel face is equal to the earth pressure at rest. The conditioned muck pressure will be increased (or decreased) in every construction phase, until blow-out (or collapse) occurs.

As shown in Figure 11, the varying of support face pressure (σ_T) (ranging from 10% to 200% of lateral earth pressure (σ_y), σ_T/σ_y)

changes the radius of action of the face. In the active and passive state, the size of the radius of action of the face is increased and the three-dimensional stress and displacement does not change. The variations were not observed to be complete between 1.5D to 2D (i.e. the plane strain condition wasn't reached). The optimal face support pressure decrease the size of the radius of action of the face.

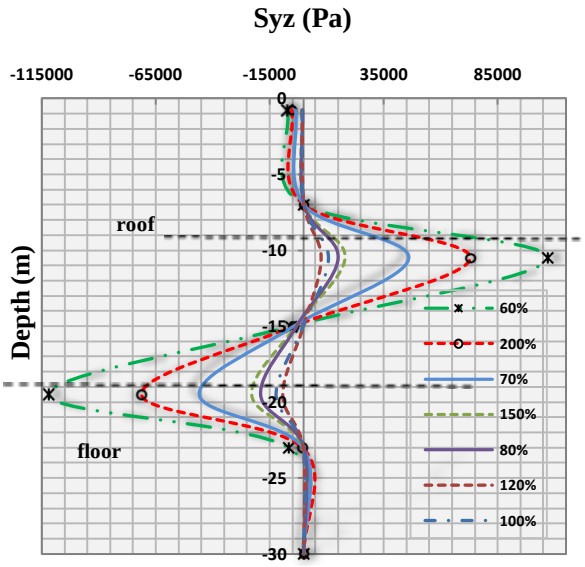

Figure 11. Contour of shear stress (Syz) at longitudinal section.

Normal stresses calculated around the tunnel face and behind the tunnel face to compare variation of normal stresses in both of face zone and stabilisation zone for varying face support pressure. Each calculation are drawn in Figure 12. The influence of different face support pressure can be pointed out. In Figure 12, the calculations lead to very similar results with perivous results in this paper.

The general three-dimensional normal stress change ahead of the working face gives a stress path which is closer to variations of shear strain rate in face zone. The opposite is true behind the face. Thus, particular care is required in performing appropriate attention to determine the radius of influence of the face.

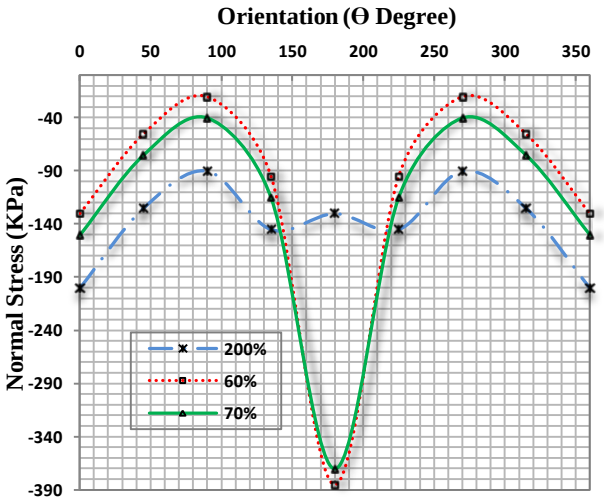

Figure. 12. Normal stresses calculated for varying face support pressure in both of face zone, stabilisation zone. (a) at face. (b) behind the tunnel face.

Figure 13 shows shear strain rate for range 100% face support pressure along the longitudinal axis at various places behind the tunnel face. Near the tunnel heading, shear strain rate is largely restricted by the optimal face support pressure. Beyond the heading, soil movement gradualy increases with distance until the plane strain condition is reached.

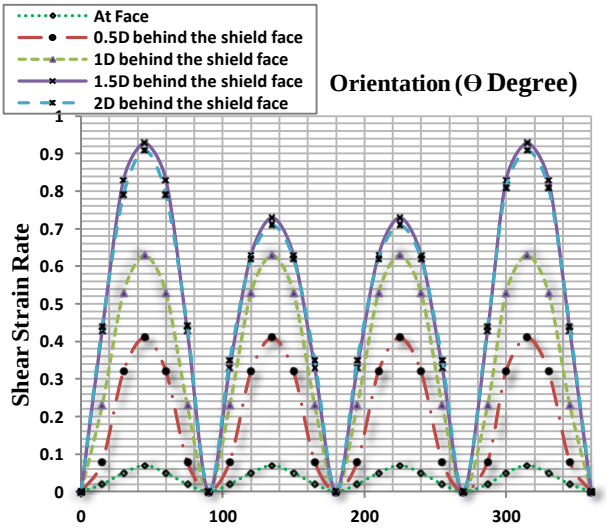

Figure. 13. Shear strain rate for range 100% face support pressure along the longitudinal axis at various places behind the tunnel face.

The shape of shear strain rate at various places behind the tunnel face (see Figure 13) are very similar, however the magnitude of shear strain reduces as the soil gets closer to the tunnel face. The maximum shear strain rate occurs at the crown level and the magnitude of shear strain rate gradually reduces as it rotates around the tunnel with minimum value occuring

at the tunnel invert. In stabilisation zone the magnitudes of shear strain rate is constant.

2 CONCLUSION

For a shield-driven tunnel advance in soft soil, the influence of the face support pressure on radius of influence of the face was analyzed numerically for shield tunneling in the metro Mashhad line 2 project. The obtained results from the conducted analyses demonstrate the complexity of the various interactions involved in shield tunneling. The conclusions obtained form this work can be summarized as below:

- This modeling procedure has the advantage of assuming the weight equilibrium of the tunnel, explaining all the phenomena of the shield tunneling, and giving a realistic estimation of the loads in the lining.
- The shear stresses (in term of Sxz and Syz) ahead of the tunnel face were examined. It is found that both the magnitude and extent of the shear stresses ahead of the tunnel heading were as significant as those behind the heading. Thus, for predicting deformation ahead of tunnel, it may be essential to know the level of anisotropy. As previously shown, anisotropy and, in particular the shear strain rate is critical for predicting movement at face and stabilization zone.
- The results of the study indicate that buildings are subjected to a wave of three dimensional displacements and strains before the tunnel reaches the plane strain condition. Thus information on displacement at the plane strain section only represents part of the required information.
- The maximum displacement occurs along the crown level. Near the tunnel heading, displacement is largely restricted by the face zone. Beyond the heading as the distance increases, soil movement gradually increases until the plane strain condition is reached. The shape of shear strain rate at various places behind the face zone are very similar,
- The distant required for the ground displacement to reach the plane strain condition will depend on the amount of plasticity developed around the tunnel face. In the active and passive state, the greater the distance behind the face that is required before the plane strain condition is reached.
- The ratio of the vertical crown displacement which occurs at the tunnel face to the crown displacement predicted by a plane strain analysis can be used as an parameter to represent the amount of three-dimensional movement which occurred ahead of the working face.

REFERENCES

Guglielmetti V, Grasso P, Mahtab A, Xu S. Mechanized tunnelling in urban areas: design methodology and construction control. Taylor and Francis; 2008. p. 507.

Itasca Consulting Group. Inc. FLAC3D Manual, third ed. (FLAC3D Version 3.1), 2006.

Jiang MJ, Yan HB, Zhu HH, Utili S. 2010, Modeling shear behavior and strain localization in cemented sands by two-dimensional distinct element method analyses. Comput Geotech, in press. doi:10.1016/j.compgeo.2010.09.001.

Kirsch A. 2010, Experimental investigation of the face stability of shallow tunnels in sand. Acta Geotech;5(1):43–62.

Li Y, Emeriault F, Kastner R, Zhang ZX. 2009, Stability analysis of large slurry shield driven tunnel in soft clay. Tunnel Underground Space Technology;24:472–81.

Renpeng C, Jun L, Xuecheng B, Yunmin C. 2009, Large scale experimental investigation on face stability of shallow tunnels in dry cohesionless soil. In: EURO: TUN 2009 – computational methods in tunnelling;. p. 809–16.

Subrin D, Branque D, Berthoz N, Wong H. 2009, Kinematic 3D approaches to evaluate TBM face stability: comparison with experimental laboratory observations. In: EURO: TUN– computational methods in tunnelling; 2009. p. 801–7.